Available online at www.sciencedirect.com
ScienceDirect
Mendeleev Commun., 2009, **19**, 96–98

Mendeleev Communications

Kinetics of the 1,3-dinitrobenzene dianion protonation with 1-butyl-3-methylimidazolium cations

Ludmila V. Mikhalchenko, Andrei S. Mendkovich,* Mikhail A. Syroeshkin and Vadim P. Gul'tyai

N. D. Zelinsky Institute of Organic Chemistry, Russian Academy of Sciences, 119991 Moscow, Russian Federation. Fax: +7 499 135 5328; e-mail: asm@free.net

DOI: 10.1016/j.mencom.2009.03.015

To estimate the applicability of 1-butyl-3-methylimidazolium (bmim$^+$) cation as an electrolyte for electrochemistry, the rate constant of the 1,3-dinitrobenzene dianion protonation with bmim$^+$ in DMF has been measured by cyclic voltammetry and chronoamperometry as 100±30 and 82±6 dm^3 mol^{-1} s^{-1} and compared with the values for phenol.

The advantages and disadvantages of room temperature ionic liquids (RTILs), in particular, the most popular 1,3-dialkylimidazolium salts, usage for researches in electroorganic chemistry were the subject of the numerous discussions in last decade.[1–3] In evaluation of applicability of the RTIL special attention should be paid to their ability to react with the primary products of the electrode reactions. Taking into account that radical anions (RA) and dianions (DA) are electrogenerated bases (EGB), the knowledge of RTIL kinetic acidity is important for their usage in electroreduction processes. However, as far as we know, the only paper on the kinetics of EGB protonation with imidazolium cations was published,[4] where the rate constant for benzophenone RA protonation has been measured. It is obvious that the evaluation of general applicability of 1-butyl-3-methylimidazolium cations (bmim$^+$) as an electrolyte requires kinetic data on proton transfer reaction between bmim$^+$ and EGB of the various natures, in particular, DA. In this work, the reaction of 1,3-dinitrobenzene (1,3-DNB) DA with bmim$^+$ has been investigated in DMF containing 0.1 M Bu_4NClO_4 by cyclic voltammetry (CV) and chronoamperometry (CA) at the carbositall electrode† to reveal the effect of bmim$^+$ concentration.

Figure 1 (dashed line) shows a CV curve of 6 mM 1,3-DNB obtained at 0.1 V s^{-1}. The empty circles are the results of digital simulation.‡ Both peaks at potentials –0.88 and –1.33 V are accounted for chemically reversible process of RA and DA formation. Figure 2 shows voltammograms of 6 mM 1,3-DNB

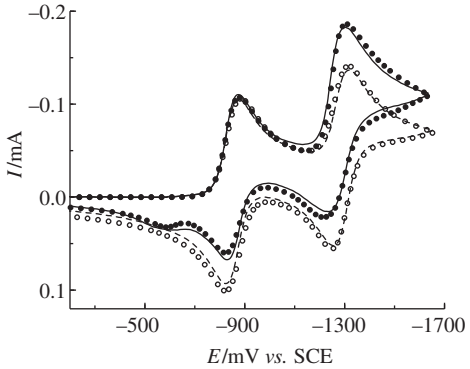

Figure 1 Cyclic voltammetry of 1,3-DNB (6 mM) in DMF (0.1 M Bu_4NClO_4) at the carbositall electrode and a potential sweep of 0.1 V s^{-1} (dashed line) and under the same conditions upon the addition of 6 mM bmim$^+$BF$_4^-$ (solid line). Empty and filled circles shows corresponding simulated curves for k = 100 dm^3 mol^{-1} s^{-1}.

† Electrochemical properties of carbositall are similar to glassy carbon.[5]

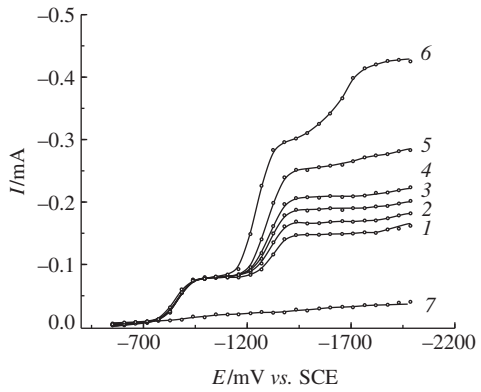

Figure 2 Voltammograms of 6 mM 1,3-DNB solutions in DMF (0.1 M Bu_4NClO_4) at the carbositall electrode containing various concentrations of bmim$^+$BF$_4^-$: (*1*) 0, (*2*) 3, (*3*) 6, (*4*) 9, (*5*) 18 and (*6*) 52 mM, (*7*) the curve for background electrolyte. The curves obtained by plotting the current values measured at various potentials by chronoamperometry at 2 s.

obtained by plotting the current values measured by CA at 2 s for various potentials. Curve *1* corresponding the reduction of 1,3-DNB in the solution free of bmim$^+$BF$_4^-$ demonstrates two waves of equal height. The current–time curves at the potentials of the limiting current of the first (i_1) and second (i_2) waves (curves *1* and *2*, Figure 3) follow the Cottrell equation with indexes of 0.500±0.007 and 0.502±0.002, which indicate that the processes are controlled by diffusion. Therefore, it may be stated that reduction of 1,3-DNB under the conditions of the experiment does not complicated by the bulk reactions of RA or DA forming at the electrode.

The addition of bmim$^+$BF$_4^-$ to the solution has virtually no effect on the shape of the first cathodic peak ($i_{p,1}$) but increases the height of the second cathodic peak ($i_{p,2}$) and decreases the height of second anodic peak (Figure 4, curve *2*). Simultaneously, a new anodic peak at potentials about –0.58 V appears. At the bmim$^+$BF$_4^-$ concentration over 16 mM, the second anodic peak

‡ Digital simulations were conducted using DigiElch Professional from ElchSoft, v. 3 (Build 3.600).[6] The standard scheme of reduction of the nitro group[7] was used in the simulation of electroreduction of 1,3-DNB with protonation of its DA as a limiting stage. The intermediate products have been synthesized and formal potentials of first and second electron transfer were measured for 3-nitrosonitrobenzene as –0.61, –1.36 and formal potential of first electron transfer for 3-nitrophenylhydroxylamine as –1.18 V. It was found, that protonation of 3-nitrosonitrobenzene DA was faster than that of DA 1,3-DNB. It was shown by CV that 3-nitrophenylhydroxylamine RA was stable at all bmim$^+$ concentrations used.

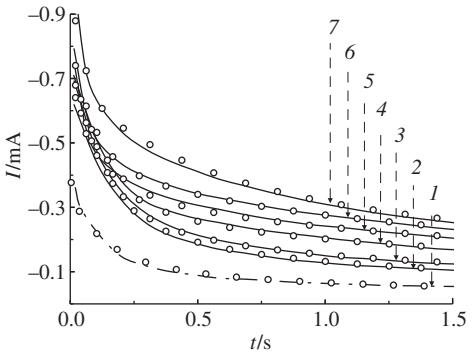

Figure 3 Simulated for $k = 82$ dm^3 mol^{-1} s^{-1} (circles) and experimental current–time curves at the potentials of the limiting current of (*1*) the first and (*2*)–(*7*) second waves of 5 mM 1,3-DNB in DMF containing 0.1 M Bu_4NClO_4. Concentrations of bmim$^+$BF$_4^-$: (*1*), (*2*) 0, (*3*) 2.4, (*4*) 8, (*5*) 16, (*6*) 27 and (*7*) 68 mM.

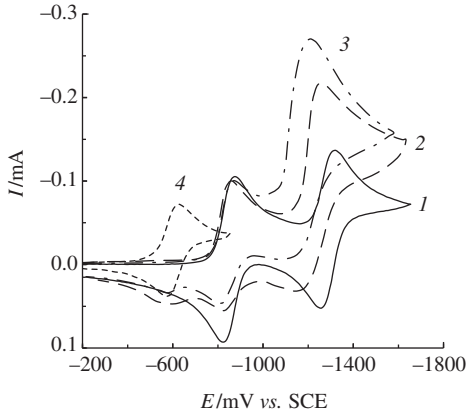

Figure 4 Cyclic voltammograms of 6 mM 1,3-DNB in DMF (0.1 M Bu_4NClO_4) at the carbositall electrode and a potential sweep of 0.1 V s^{-1}: (*1*) no addition; addition of (*2*) 18 mM bmim$^+$BF$_4^-$ and (*3*) 18 mM phenol. (*4*) Cyclic voltammogram of 5 mM 3-nitrosonitrobenzene.

disappears completely and another new broad anodic peak at a potential of about –1.14 V may be observed (Figure 4, curve *2*).

Similar changes in the shape of the CV curve of 1,3-DNB are observed when phenol is added to the solution (Figure 4, curve *3*). The addition of ethanol and *tert*-butanol affects the shape of the curve similarly but this change appears only at alcohol concentrations 25 to 30-fold higher than that of bmim$^+$. Similarity of the effects demonstrates that the bmim$^+$ react with DA 1,3-DNB by the same way as such OH proton donors do. The formation of 3-nitrophenylhydroxylamine RA was observed earlier in electroreduction of 1,3-DNB in DMF solution containing phenol.[8]

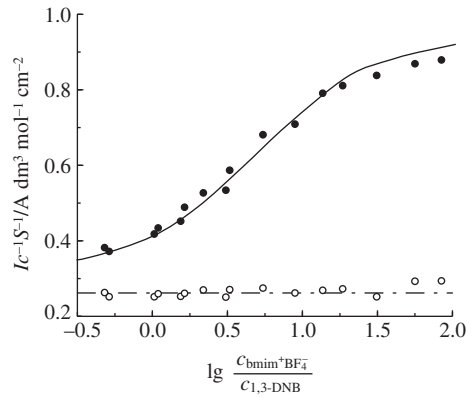

Figure 5 Dependences of the first (empty circles) and second (filled circles) cathodic peaks currents at voltammograms of 1,3-DNB on the concentration ratio of bmim$^+$BF$_4^-$ to 1,3-DNB. Solid and dash-dotted lines show corresponding theoretical dependences for $k = 100$ dm^3 mol^{-1} s^{-1}.

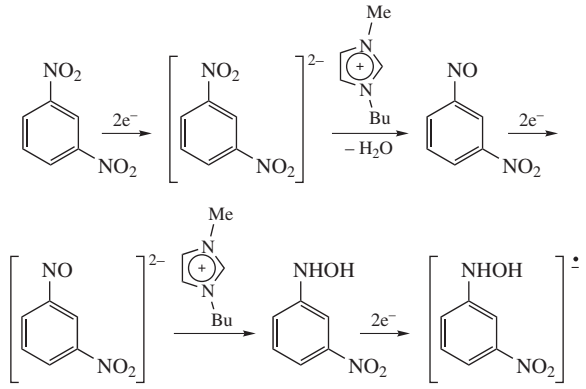

Scheme 1

The dependence of $i_{p,2}$ on the logarithm of concentration ratio of bmim$^+$BF$_4^-$ to 1,3-DNB has *S*-like pattern and reaches the limit at ratio values about 18 (Figure 5). The limiting value of $i_{p,2}$ corresponds the theoretical value for a five-electron process described by Scheme 1.

A plot of $i_{p,2}$ *vs.* square root of sweep rate ($v^{1/2}$) demonstrates leanearity in the absence of bmim$^+$BF$_4^-$, but splits in two linear parts in the presence of bmim$^+$ (Figure 6, curve *2*). At low sweep rates, the slope of curve *2* is remarkably larger than that in the absence of bmim$^+$BF$_4^-$ (curve *1*). At high sweep rates, slopes of both curves at Figure 6 become practically equal. This may be treated as an indication of transition from kinetic multi-electron current to diffusion two-electron process. The value of $v^{1/2}$ corresponding to the slope change point increases with increasing of bmim$^+$ concentration. Figure 6 shows that experimental values of $i_{p,2}$ lay at the theoretical curves obtained by simulation.

Using the experimental values of $i_{p,2}$ at various concentration ratios of bmim$^+$BF$_4^-$ to 1,3-DNB (Figure 5), the rate constant of dianion protonation may be estimated as 100±30 dm^3 mol^{-1} s^{-1}.[§] However, it should be taken into account that peak currents are affected not only by kinetics of the bulk reactions but also by heterogeneous kinetics. Moreover, the potential scanning results in complicate evolution of the intermediate species concentration profiles and may require to complicate seriously the kinetic scheme used. Therefore, we use CA as a main method for the kinetic investigations of the dianion 1,3-DNB protonation by bmim$^+$.

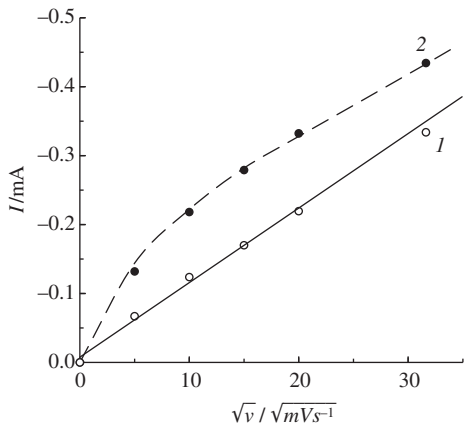

Figure 6 (*1*) A plot of $i_{p,2}$ *versus* square root of sweep rate ($v^{1/2}$) for 5 mM solutions of 1,3-DNB in DMF (0.1 M Bu_4NClO_4). (*2*) The same solution containing 15 mM bmim$^+$BF$_4^-$. Dashed line show theoretical curve at $k = 100$ dm^3 mol^{-1} s^{-1}.

[§] The values of rate constant of DA protonation (k) were calculated from the experimental values of $i_{p,2}$ and i_2 measured for various concentration ratios of bmim$^+$BF$_4^-$ to 1,3-DNB (R_c), according to simulated reference dependences $i_{p,2} = f(k, R_c)$ and $i_2 = f(k, R_c)$.

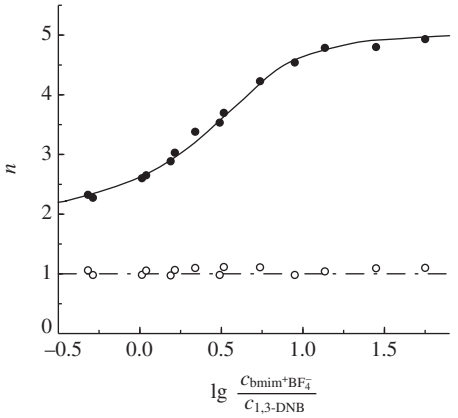

Figure 7 Dependence of the apparent number of electrons involved in the electroreduction at the first (empty circles) and second (filled circles) steps of reduction, measured by chronoamperometry at $t = 1$ s, on the ratio of concentrations of $bmim^+BF_4^-$ and 1,3-DNB. Solid and dash-dotted lines show corresponding theoretical dependences for $k = 82$ dm^3 mol^{-1} s^{-1}.

Figures 2 and 7 give an example of i_1 and i_2 dependence on $bmim^+BF_4^-$ concentration.¶ Similar to described above dependence (Figure 5) i_1 value keeps constant when i_2 increases with increasing of concentration ratio of $bmim^+BF_4^-$ to 1,3-DNB (Figure 7) and reaches limiting value at 40–50 mM. Figure 7 shows that apparent number of electrons†† (n) at the limit is also close to 5 as it was in case of $i_{p,2}$. The rate constant of DA protonation estimated with the data obtained by CA (Figure 7) equals 82±6 dm^3 mol^{-1} s^{-1}. This value is about 20% lower than that obtained by CV, but the last should be treated as less reliable and less precise by the reasons discussed above. The obtained values of k are rather close to that of phenol.[9]

Unlike $bmim^+BF_4^-$, the introduction of 1-butyl-2,3-dimethylimidazolium tetrafluoroborate into the solution exerts virtually no effect on the height of the cathodic peaks, inducing only its shift toward positive potentials. This allows one to suggest that protonation of dianion 1,3-DNB by $bmim^+$ involves the proton located at the 2-position of imidazole ring. In turn, this means that the protonation should be accompanied by carbene formation.[10]

¶ Note that at high concentration of $bmim^+BF_4^-$ the measurements of i_2 are embarrassed because of third wave development (Figure 2, curve *6*).

†† This value was obtained as result of division of i_1 and i_2 by theoretical values for diffusion process.

References

1 *Electrochemical Aspects of Ionic Liquids*, ed. H. Ohno, Wiley & Sons, Inc., Hoboken, New Jersey, 2005.
2 Ph. Hapiot and C. Lagrost, *Chem. Rev.*, 2008, **108**, 2238.
3 J. Zhang and A. M. Bond, *Analyst*, 2005, **130**, 1132.
4 S. O'Toole, S. Pentlavalli and A. P. Doherty, *J. Phys. Chem. B*, 2007, **111**, 9281.
5 S. E. Panicheva and B. K. Filanovskii, *Zavodskaya Laboratoriya*, 1989, **55** (5), 23 (*Industrial Laboratory*, 1989, **55**, 519).
6 http://www.elchsoft.com/DigiElch/Default.aspx
7 H. Lund, in *Organic Electrochemistry*, 4th edn., eds. H. Lund and O. Hammerich, Marcel Dekker, New York, 2001, ch. 9.
8 H. Wang and V. D. Parker, *Acta Chem. Scand.*, 1994, **48**, 933.
9 M. A. Syroeshkin, A. S. Mendkovich and L. V. Mikhalchenko, *Abstracts of Symposium 'Modern Chemical Physics'*, Tuapse, 2007, p. 267.
10 S. Chowdhury, R. S. Mohan and J. L. Scott, *Tetrahedron*, 2007, **63**, 2363.

Received: 2nd October 2008; Com. 08/3222